UNLOCKING INSIGHTS: MASTERING EXTRACELLULAR VESICLE FLUORESCENCE LABELING AND ANALYSIS WITH NANOSIGHT PRO

Methods and best practice for nanoparticle tracking analysis

In this white paper, we present methods developed for fluorescence labeling and detection of extracellular vesicles (EVs) using the NanoSight Pro, alongside representative data to guide the implementation of these methods.

We utilized EVs sourced from urine, assessing their size distribution and concentration through light scatter and fluorescence analysis. Employing a diverse array of fluorescent dyes and fluorophores, we not only confirmed the presence of EVs but also effectively detected tetraspanin biomarkers on their surface and internal RNA cargo.

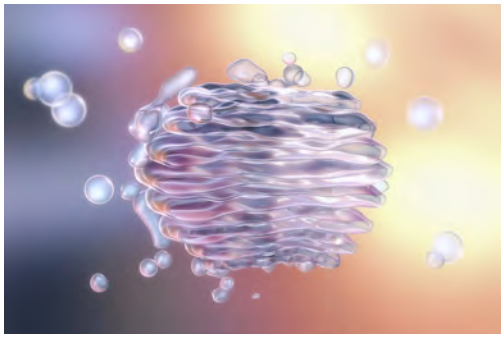

1.0 Introduction

Ongoing exploration of extracellular vesicles (EVs) has ignited growing interest driven by their evolving applications and breakthroughs, particularly in the areas of disease diagnosis and therapeutic potential [1]. These microscopic biologics generated by cells within living organisms were initially thought to be cellular waste. However, research has unveiled their crucial role in intercellular communication.

Extracellular vesicles is a general term and many EV subtype definitions are used, including classification based on their size range: small EVs (<200nm) and large EVs (>200nm). Exosomes represent a subtype of small EVs and are related to EVs that originated from the plasma membrane [2].

Extracellular vesicles extracted from body fluids are accompanied by non-EV components creating quite a diverse and heterogeneous system that poses significant challenges for analytical characterization [2]. Important EV characteristics included size and size distribution, which can be informative of their origin and effectiveness of purification methods. The change in concentration of released EVs can be indicative of an increase in communication, and this has diagnostic potential [5]. Accurately characterizing the size, heterogeneity, and concentration of EV preparations yields essential information for profiling, understanding biological function, and diagnosing conditions.

EVs contain various molecules such as proteins, lipids, and nucleic acids (including RNA and DNA). The composition of EVs, including their cargo molecules, can reflect the physiological or pathological state of the cell they originated from. This characteristic makes EVs promising biomarkers for a spectrum of diseases, ranging from cancer to neurodegenerative disorders and inflammatory conditions. [4]. To date, there are no accepted universal molecular markers of EVs or EV subtypes [2]. Although not common in all EVs, notable biomarkers heavily used in research are the tetraspanins (including CD9, CD81 and CD63) as they accumulate on the small EVs' surface as opposed to cell lysates [5]. The tetraspanins are integral trans-membrane proteins intricately involved in various aspects of extracellular vesicle biology, including biogenesis, cargo sorting, and interaction with recipient cells. Due to their high abundance on the surface of many EV subsets, they are

considered the most accessible biomarkers for research, often utilized in EV profiling and as specific exosome markers. Thus, the ability to detect these biomarkers holds considerable importance in EV research [6].

Additionally, the ability to detect and quantify RNA within EVs is equally crucial, as it offers valuable insights into their diagnostic potential and the success of encapsulation for therapeutic applications. Assessing the RNA cargo can shed light on EVs' functional roles in intracellular communication and disease processes, while also serving standardization and quality control purposes [7].

2.0 NanoSight NTA

Due to the complex nature of EVs, a multi-technology approach is often applied to fully characterize the EVs including flow cytometry, western blotting, enzyme-linked immunosorbent assays (ELISA), mass spectrometry proteomics, microscopy-based methods and nanoparticle tracking analysis (NTA) [8], [9], [2]. NTA has become a commonly used technique for rapid characterization of high-resolution size and concentration of extracellular vesicles [10].

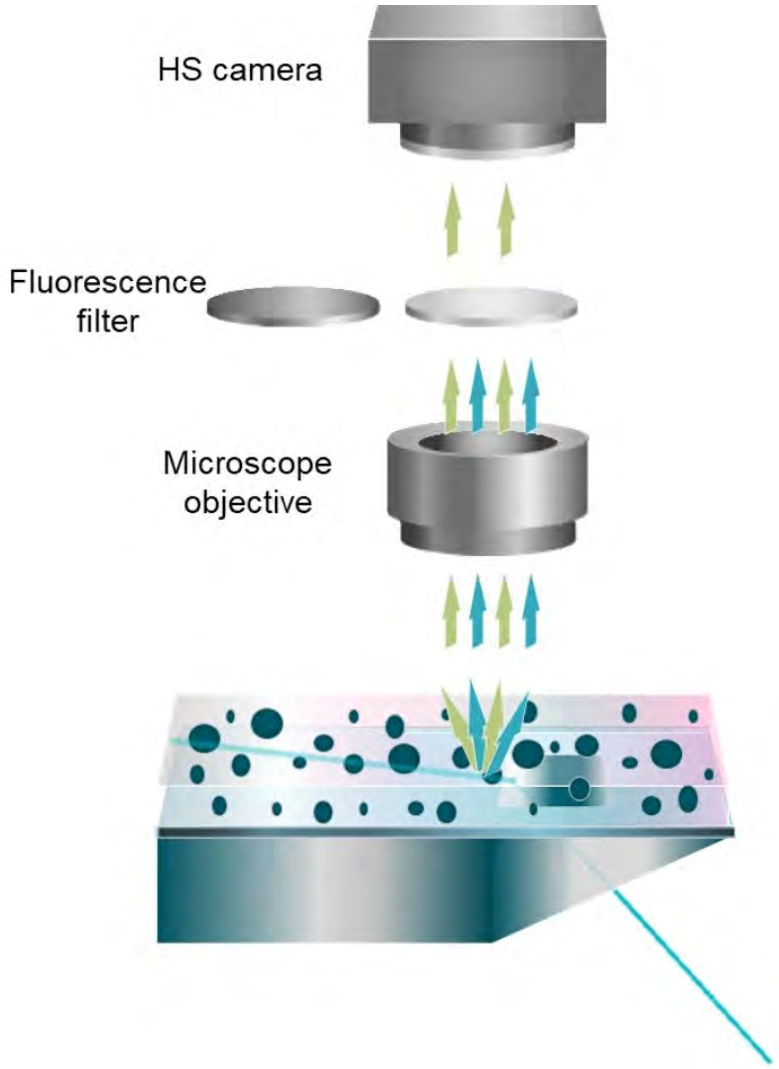

Figure 1: Schematic of NTA optical setup

NanoSight NTA uses a laser to illuminate the particles and an optical microscope configuration to capture the light scattering from particles. By tracking their Brownian motion and applying the Stokes-Einstein equation NanoSight can determine the particles' hydrodynamic diameter. The concentration is derived from the particle count. NanoSight Pro has additional fluorescence capabilities, where specific laser excitation prompts emitted fluorescence wavelengths to reach the detector through a matching long-pass optical filter. Additionally, the laser is intermittently deactivated, and fresh sample is introduced between measurements to mitigate the effects of photobleaching. These novel features, combined with the trained neural network for particle identification [11] and the continuous and controlled pumping of samples during the measurement, are essential for enhancing and ensuring the quality of fluorescence detection.

Fluorescent NTA provides deeper insights into samples and enables subpopulations to be distinguished. This capability is becoming increasingly vital for EVs research, to assess purification efficiency, and confirm the presence of specific markers or cargo in exosome samples [12].

3.0 Materials and Methods

3.1 Reagents

This study uses EVs in the form of lyophilized exosomes from the urine of healthy donors from HansaBioMed Life Sciences (Cat # HBM-PEU). These exosomes express tetraspanins CD9, CD63 and CD81 confirmed previously by western blot and flow cytometry [13].

The exosomes were tagged via membrane, specific biomarker and RNA labeling. This study presents the final method for each labeling.

CellMask™ Orange Plasma Membrane Stain (Cat # C10045, Invitrogen™) and ExoGlow™-NTA Fluorescent Labeling Kit (Cat # EXONTA200A-1, System Biosciences) were used for labeling the EVs' membranes.

For biomarker detection via direct antibody labeling, Alexa Fluor® 488 and PE/Cyanine7 fluorescent antibodies were used to label CD9, CD63 and CD81 tetraspanins. Alexa Fluor™ 488 anti-human CD9 Monoclonal Antibody (MEM-61) (Cat # MA5-44126) and Alexa Fluor™ 488 anti-human CD81 Monoclonal Antibody (M38) (Cat # MA5-44132) were purchased from Invitrogen™. Alexa Fluor® 488 anti-human CD63 Antibody (Cat # 353037), PE/Cyanine7 anti-human CD9 Antibody (Cat # 312115), PE/Cyanine7 anti-human CD63 Antibody (Cat # 353009) and PE/Cyanine7 anti-human CD81 (TAPA-1) antibody (Cat # 349511) dyes were purchased from Biolegend. Quant-iTTM RiboGreen RNA Kit (Cat # R11491, containing RNA reagent and TE buffer) was purchased form Invitrogen™ and was used to label RNA inside the exosomes.

All samples were prepared in either phosphate-buffered saline (PBS), pH 7.4 (1X) (Cat # 10010023, Gibco™) or deionised particle-free water (Milli-Q).

3.2 Preparation of EVs

The lyophilized exosomes were reconstituted in deionized water (Milli-Q) by adding 100 µl MilliQ water to the 100 µg sample (Figure 2), and gentle pipette mixing to generate an exosome stock, with a concentration of approximately 1×10^{12} particles/mL.

All samples were prepared and measured across various days using the same exosomes stock material. Since volumetric dilution was employed for all sample preparations the likelihood of introducing dilution errors increased, thereby resulting in variations in the reported sample concentration values.

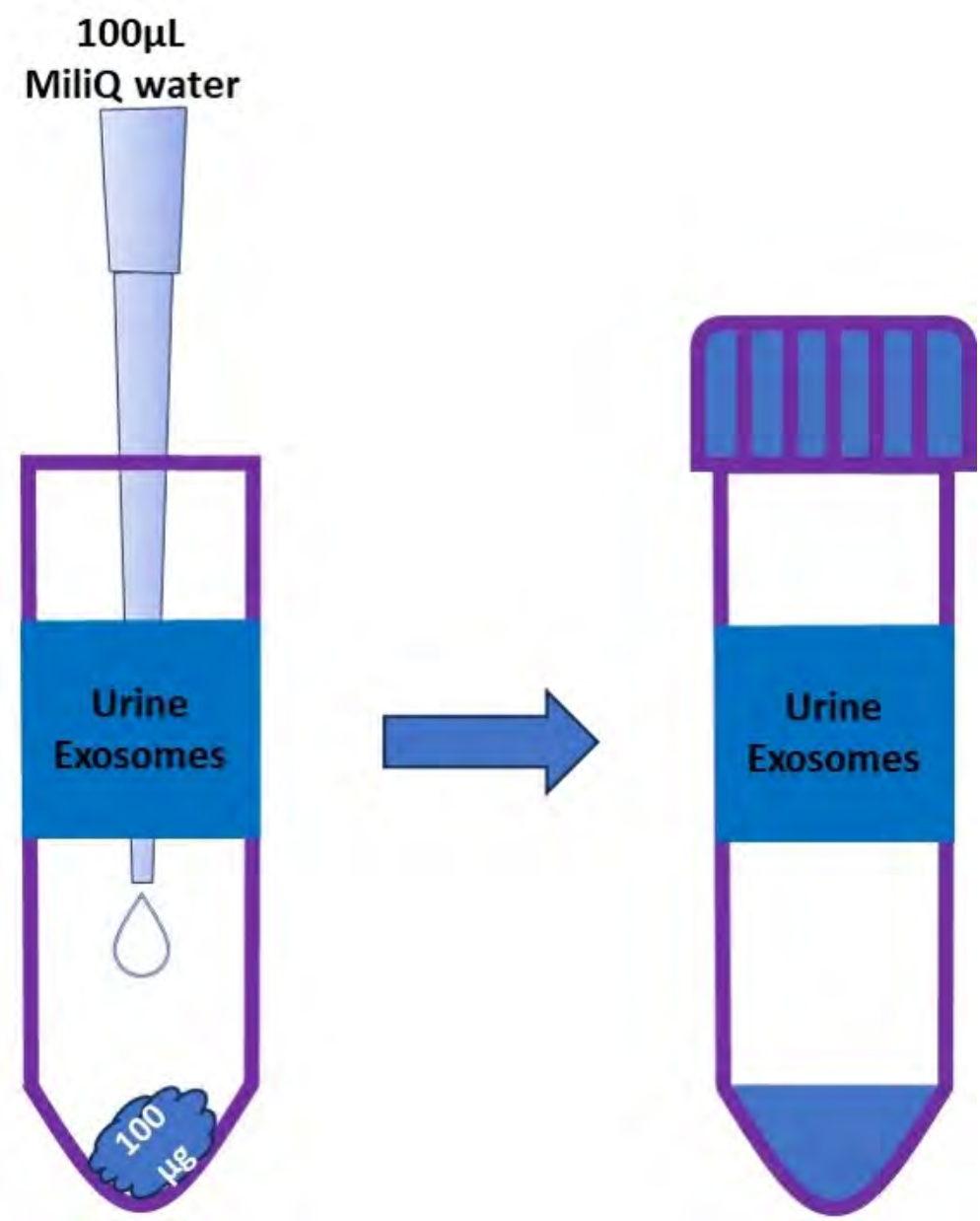

Figure 2: Schematic showing reconstitution of exosomes from urine

3.2.1 Control Exosomes

The exosome stock was diluted volumetrically by a factor of 5000 using serial dilution in filtered phosphate-buffered saline (PBS, 1X) to a final concentration of approximately 2 – 5 × 10^8 particles/mL, a suitable concentration for NTA measurements (Figure 3). This concentration variation is due to dilutions being performed volumetrically and on different days. Unlabeled controls were prepared under identical conditions and on the same day and time as the respective labeled samples.

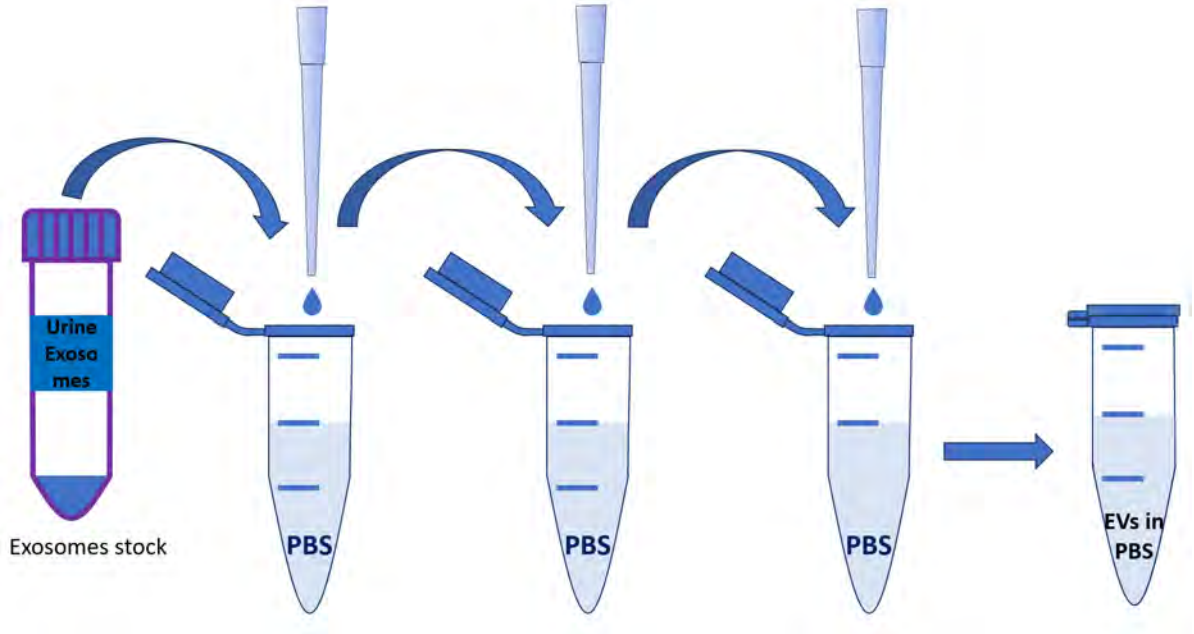

Figure 3: Schematic showing volumetric three-step serial dilution of exosomes from urine to a suitable concentration for NanoSight Pro measurements to be used as a non-fluorescent control

3.2.2 Membrane labeling

EVs containing lipid bilayer in their structure are great candidates for utilizing membrane dyes to tag their lipidic membrane. Using a general membrane to label EVs is relatively simple and the emitted fluorescence signal from stained EVs is usually very effective as the dye easily penetrates and incorporates into a lipid bilayer in high volumes. [14]. Although membrane labeling is not specific due to dye sensitivity to other plasma or lipidic non-EV components, it is often utilized as a first step in the generic description of purified samples to confirm the presence of EVs in enriched preparation. CellMask™ Orange (CMO) and ExoGlow™ were used and both labeling protocols are shown below.

3.2.2.1 Membrane labeling with CellMask™ Orange (CMO)

CellMask™ Orange (CMO) Plasma Membrane Stain was diluted by a factor of 10,000 in PBS using serial dilution to create a CMO dye stock of 5 µg/ml concentration (Figure 4B). The exosome stock was diluted by a factor of 10 in PBS to create exosome working stock A (Figure 4A). Equal volumes (10 µl) of the CMO dye stock and exosome working stock A were added to an Eppendorf tube, gently mixed by pipetting and left to react for 20 minutes at room temperature in the dark (Figure 4C). The exosome-dye mixture was then diluted with PBS by a further factor of 500 to final exosome's concentration suitable for NTA measurements (Figure 4D).

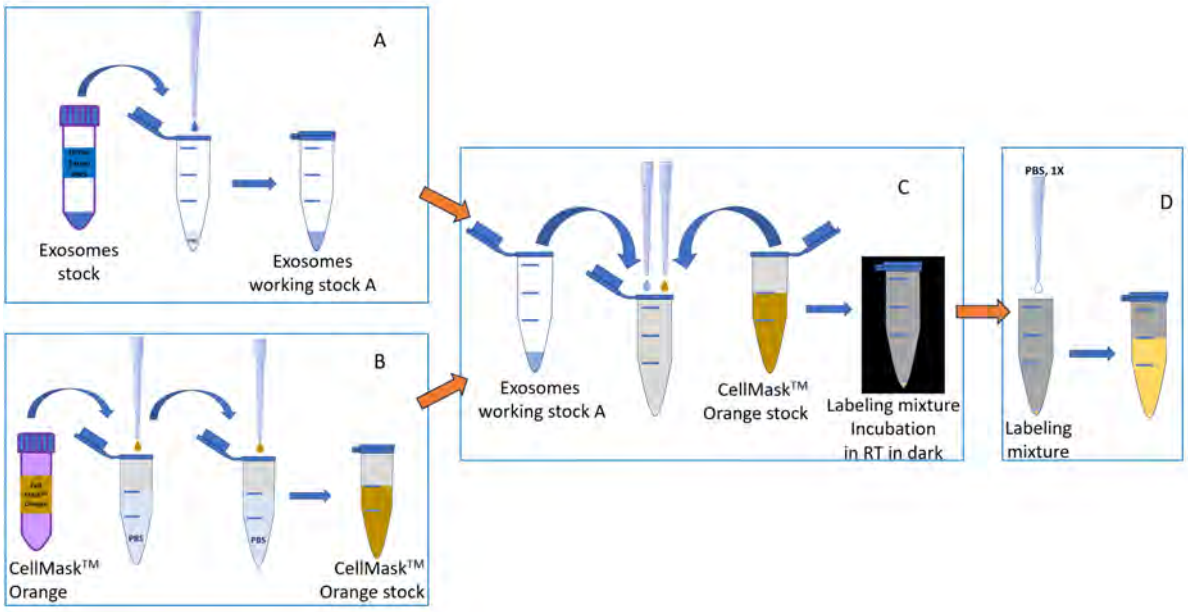

Figure 4: Schematic showing the steps of exosomes from urine labeling with CellMaskTM Orange (CMO). A – Preparation of Exosomes working stock A, B - Preparation of CMO stock, C -Preparation of labeling mixture and its incubation, D - final dilution of the CMO labeled exosomes

3.2.2.2 Membrane labeling with ExoGlow™

ExoGlow™-NTA fluorescent labeling dye was diluted by a factor of 10 in PBS to create an ExoGlow™ dye stock (Figure 5B). The exosome stock was diluted by a factor of 5 in PBS to create exosome working stock B (Figure 5A). Equal volumes (10 µl) of the ExoGlow™ dye stock and exosome working stock B were added to an Eppendorf tube, gently mixed by pipetting and left to react for 20 minutes at room temperature in the dark (Figure 5C). The exosome-dye mixture was then diluted with PBS by a further factor of 1000 to final exosome's concentration suitable for NTA measurements (Figure 5D).

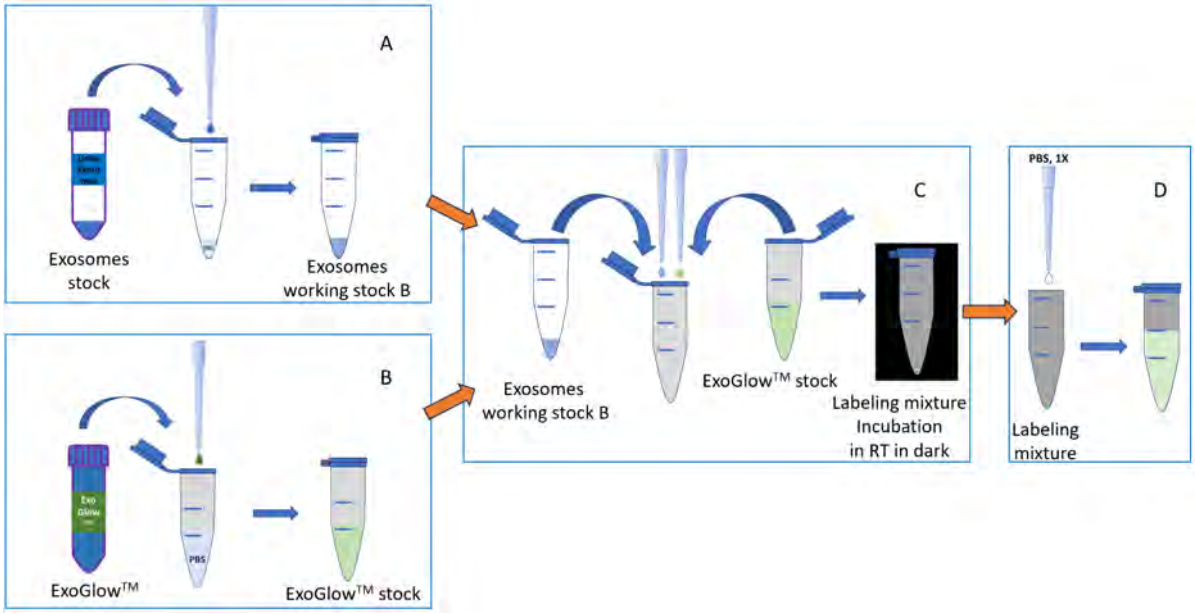

Figure 5: Schematic showing the steps of exosomes from urine labeling with ExoGlowTM. A – Preparation of Exosomes working stock B, B - Preparation of ExoGlowTM stock, C -Preparation of labeling mixture and its incubation, D - final dilution of the ExoGlowTM labeled exosomes.

3.2.3 Biomarker tetraspanin labeling

CD9, CD63 and CD81 are used as exosome identifiers, thus detecting the presence of these tetraspanins can provide information on the exosome origin. The exosomes used in this study had the presence of the CD9, CD63 and CD81 markers confirmed by the manufacturer in the product specifications [15]. Primary antibody labeling was used to tag the biomarkers on the exosomes' surface. This method involves the use of antibodies conjugated to a fluorophore, enabling direct recognition and binding to the antigen of interest on the exosome surface. Two different fluorophores (Alexa Fluor® 488 and PE/Cyanine7) were used, each linked with 3 different antibodies against tetraspanin markers: anti-CD9, anti-CD63 and anti-CD81. The protocols for both fluorophores are shown below.

3.2.3.1 Tetraspanin labeling with Alexa Fluor® 488 antibody

The anti-human CD9 Alexa Fluor® 488 antibody, anti-human CD63 Alexa Fluor® 488 antibody and anti-human CD81 Alexa Fluor® 488 antibody dyes were initially diluted by factors of 50 in PBS to create three fluorescent antibody stocks (Figure 6B1, 6B2 and 6B3). For each antibody dye stock, 10 µl was taken and added to different Eppendorf tubes. Equal volumes (10 µl) of exosome working stock B (prepared as presented in section 3.2.2.2) (Figure 6A) were also added to each tube, gently mixed by pipetting and left to react for 30 minutes at room temperature in the dark (Figure 6C1, 6C2 and 6C3). Each exosome-antibody dye mixture was then diluted with PBS by a further factor of 500 to the final exosome's concentration suitable for NTA measurements (Figures 6D1, 6D2 and 6D3).

3.2.3.2 Tetraspanin labeling with PE/Cyanine7 antibody

The PE/Cyanine anti-human CD9 antibody, PE/Cyanine anti-human CD63 antibody and PE/Cyanine anti-human CD81 antibody were initially diluted in PBS to create three fluorescent antibodies stocks, diluting by factors of 10, 10 and 40 respectively (Figure 6B1, 6B2 and 6B3). For each antibody dye stock, 10 µl was taken and added to different Eppendorf tubes. Equal volumes (10 µl) of exosome working stock B (prepared as presented in section 3.2.2.2) (Figure 6A) were also added to each tube, gently mixed by pipetting and left to react for 30 minutes at room temperature in the dark (Figure 6C1, 6C2 and 6C3). Each exosome-antibody dye mixture was then diluted with PBS by a further factor of 500 to final exosome's concentration suitable for NTA measurements (Figure 6D1, 6D2 and 6D3) as also presented in section 3.2.3.1.

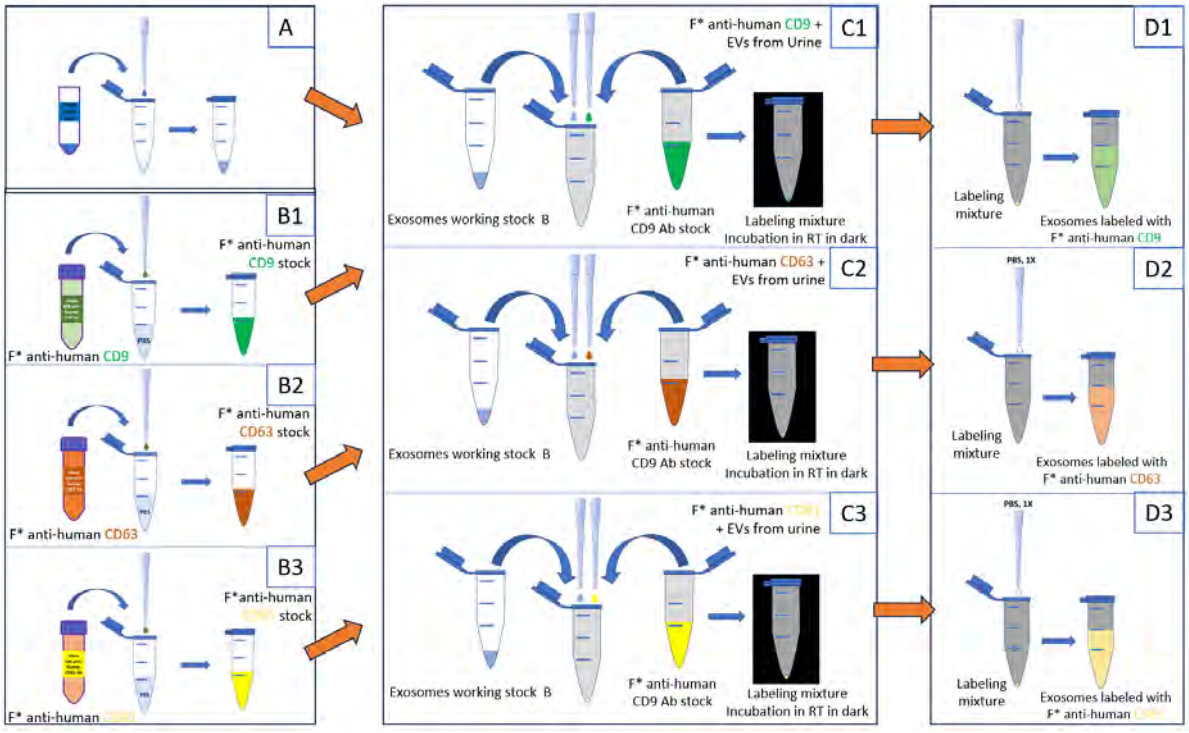

Figure 6: Schematic showing the steps of exosomes from urine labeling with primary anti-human CD9, anti-human CD63 and anti-human CD81 Antibodies linked to Fluorophore (F). F* represents fluorophore. A – Preparation of Exosomes working stock B, B - Preparation of F* anti-human (CD9, CD63 and CD81) Antibody stock, C1-C3 -Preparation of labeling mixtures and their incubation, D1-D3 - final dilution of the F* anti-human (CD9, CD63 and CD81) labeled exosomes*

3.2.3 RNA labeling

Exosomes mediate cellular communication with their cargo, often a form of RNA. As the RNA is enclosed inside of the exosomes, it is quite challenging to characterize this component without destroying exosomes. In this paper, we demonstrate the novel approach for RNA labeling inside the EVs. Quant-iT™ RiboGreen was selected as this RNA-specific dye is used for its quantification in a solution. Here, we utilize the reagent to detect RNA-EVs in exosomes from urine preparation.

3.2.3.1 RNA labeling with Quant-iT™ RiboGreen

Quant-iT™ RiboGreen was diluted by a factor of 25 in 20x TE buffer (included in the labeling kit) to create a dye stock (Figure 7B). The exosome stock was diluted by a factor of 100 in PBS to create an exosome working stock C (Figure 7A). Equal volumes (20 µl) of the dye stock and exosome working stock C were added to an Eppendorf tube, gently mixed by pipetting and left to react for 30 minutes at room temperature in the dark (Figure 7C). The exosome-dye mixture was then diluted with deionized water by a further factor of 50 to final exosome's concentration suitable for NTA measurements (Figure 7D).

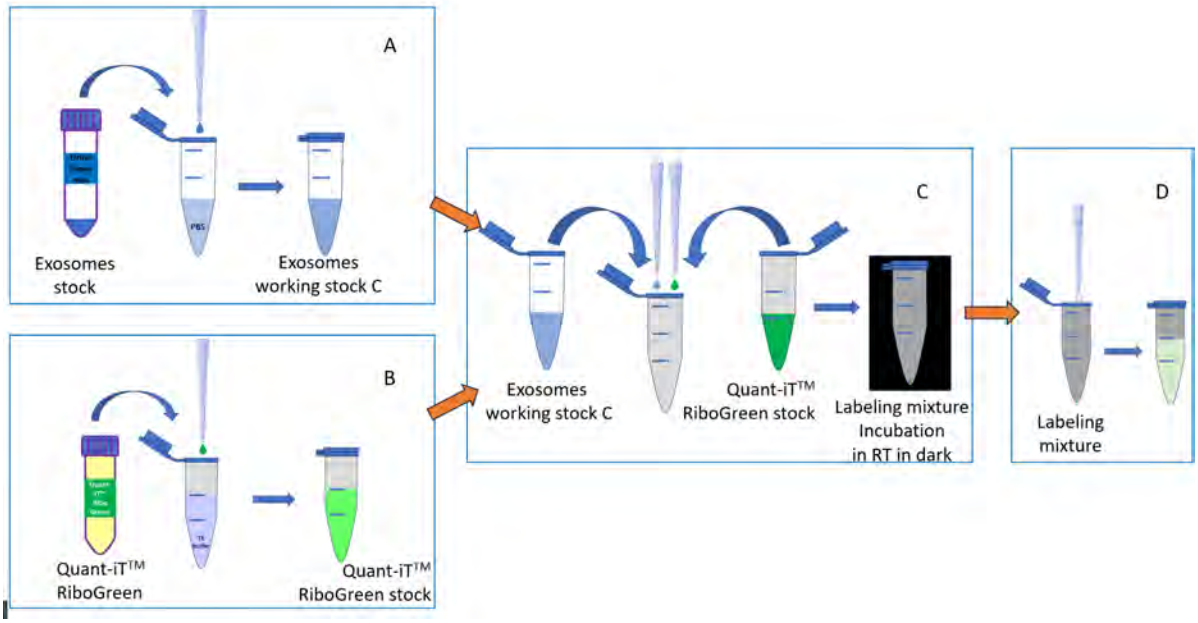

Figure 7: Schematic showing the steps of exosomes RNA labeling with Quant-iT™ RiboGreen. A – Preparation of Exosomes working stock C, B - Preparation of Quant-iT™ RiboGreen, C -Preparation of labeling mixtures and their incubation, D - final dilution of the Quant-iT™ RiboGreen - RNA labeled exosomes.

3.3 Nanoparticle Tracking Analysis (NTA)

Nanoparticle Tracking Analysis (NTA) measurements were performed on the NanoSight Pro equipped with 488 nm and 532 nm lasers using NS Xplorer software (version 1.0).

The appropriate laser wavelengths and fluorescent long-pass filters were applied for each fluorescent measurement according to the dyes excitation and emission properties as shown in Table 1 [16], [17], [18], [19], [20]. PE/Cyanine7 has a very broad excitation spectra meaning multiple wavelengths can be used to induce/trigger fluorescence. The 488 nm laser was chosen for PE/Cyanine7 labeled exosomes as this wavelength produced the strongest NTA fluorescence signal.

Fluorescent dye	Fluorophore Excitation max	NanoSight Pro Laser wavelength [nm]	Fluorophore Emission Max	NanoSight Pro long pass Fluorescent filter [nm]
CellMask™ Orange	556	532	571	565LP
ExoGlow™	465	488	635	500LP
PE/Cyanine7	565	488/532	778	500LP/565LP
Alexa Fluor® 488	496	488	519	500LP
Quant-iT™ RiboGreen	500	488	525	500LP

Table 1: Fluorescent dyes and corresponding excitation wavelengths and long pass filters required for fluorescence NTA measurements

The NS Xplorer software has an integrated fluorescence mode that performs the combined analysis of light scatter and fluorescence within a single measurement, reporting not only size distributions but also concentrations and fluorescence efficiency directly. The fluorescence efficiency compares concentration measured with and without a fluorescence filter within a single experiment, providing a percentage of particles in the sample that are fluorescent.

For a comprehensive fluorescence analysis, the default settings of 10 captures with a duration of 150 frames each were utilized for both the light scatter and fluorescence parts. The automatic camera and focus setup were used for the scatter part of measurements, whereas the manual camera and focus settings were used in the fluorescence part. For fluorescence, the highest camera settings were used (exposure time = 40 ms, contrast gain = 15.8). All samples were measured in a flow of approximately 5 µl/min. For consistency and comparison purposes, all sample controls were analysed using the same fluorescence method. In NS Xplorer, the data is processed automatically using machine-learning trained algorithm for particle detection [11], where no user input is required, removing user bias leads to the generation of more reproducible data.

The representation of the data is shown for each labeling. The mode of the raw size distribution was recorded as the size parameter of the extracellular vesicles (diameter, nm). The concentration and fluorescence labeling efficiency were also determined by the NS Xplorer software.

4.0 Results & Discussion

4.1 Control Exosomes

The control EVs were measured using both the 488 nm and 532 nm lasers with their corresponding long pass filters of 500 nm and 560 nm, respectively. As expected, samples were successfully analyzed in the light scatter, and no fluorescence signal from unlabeled EVs was detected with both lasers and their corresponding LP filters.

The EVs displayed no autofluorescence and no fluorescence distribution was generated resulting in a 0% fluorescence efficiency. Figure 8 shows the size distribution of the exosomes, representing a typical heterogenous distribution, often expected for biological samples.

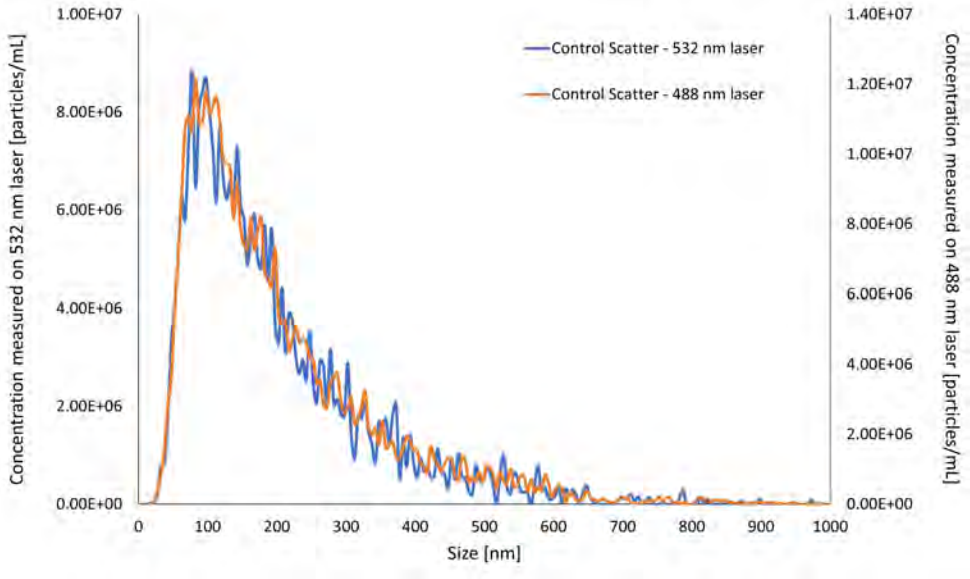

Figure 8: Scatter size distribution of exosomes from urine control measured on 488 nm laser with 500 nm long pass filter (orange) and 532 nm laser with 560 nm long pass filter (blue)

Concentrations of 3.9×10^8 particles/mL and 4.5×10^8 particles/mL and modal size of 77.5 nm and 82.5 nm were measured using the 532 nm and 488 nm lasers respectively. Given the inherent heterogeneity of exosomes and the fact that these measurements were conducted on various days, variability in their concentrations was observed. However, the size distribution profiles remained consistently similar in shape. Also, as the samples were diluted volumetrically, some level of variation in concentration was also expected and fell within the expected error range for this dilution method. It is best practice to carry out a control measurement for NTA ideally on the same day as the labeled sample, to confirm whether the addition of fluorophores affects the intrinsic properties of the sample.

4.2 Membrane Labeling

As generic CMO and ExoGlow™ dyes easily integrate into the EV membranes, the overall EV concentration can be determined with and without a fluorescent filter (Carnell-Morris et al., 2017 [14]), [21]. Both dyes showed high ~100% fluorescence efficiency indicating all particles within the sample preparation were fluorescently labeled (102% for CMO and 96% for ExoGlow™).

The scattering and fluorescent size distributions for both CMO and ExoGlow™ labeling are shown in Figure 9. For both dyes, the scatter and fluorescence size distributions share the same shape and overlay showing that the entire sample size distribution range has been successfully labeled. The distributions of the labeled exosomes also closely fit the EV control distribution showing that the labeling process had not affected the original size and concentration of the exosomes.

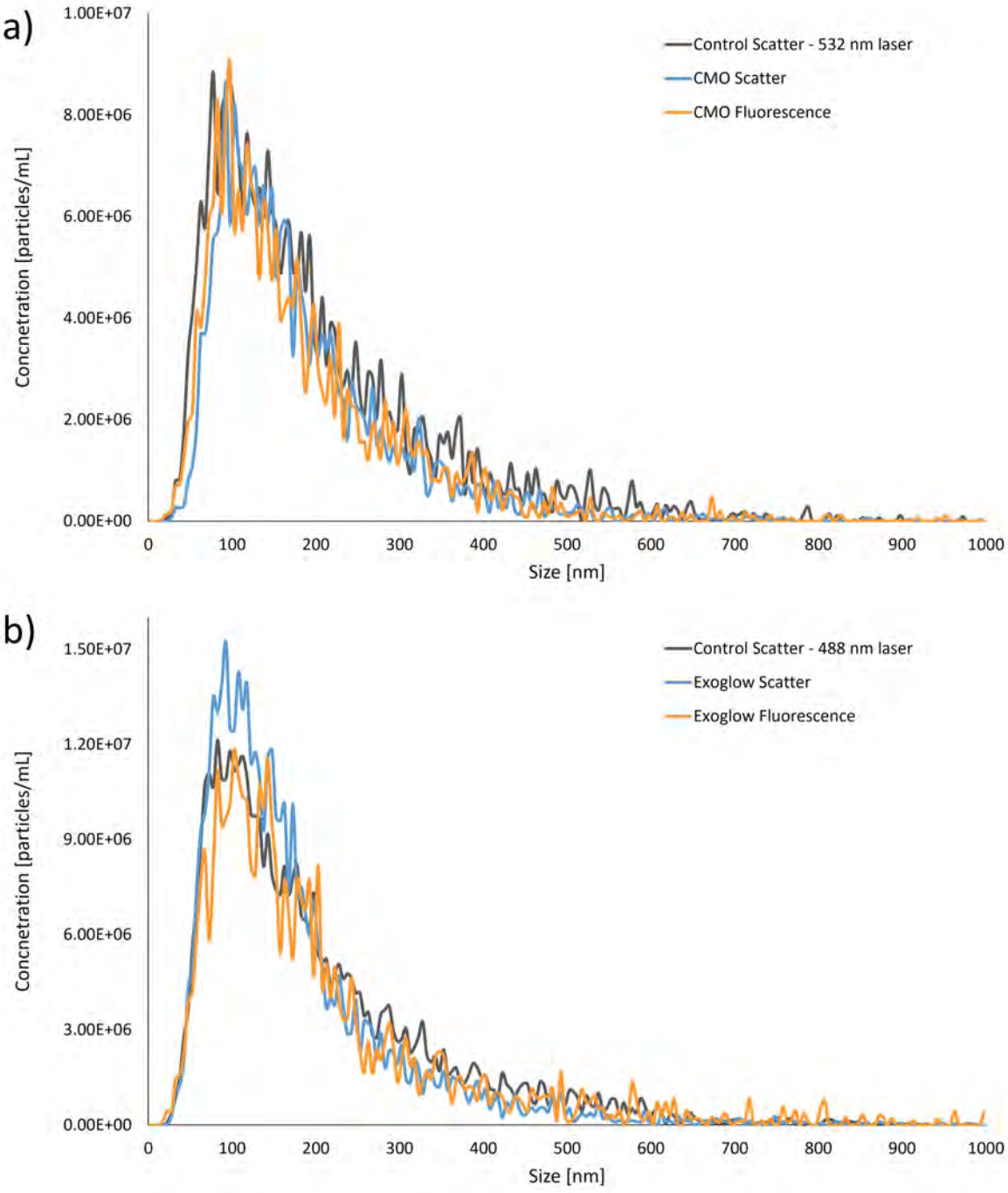

Figure 9: Scattering (blue) and fluorescence (orange) size distribution of exosomes from urine of healthy donors labeled with a) CMO and b) ExoGlow™ membrane dyes. The unlabeled control EVs size distribution is shown in black.

The modal size and particle concentration data for membrane-labeled EVs are shown in Table 2. The differences in the reported concentration and size between the two dyes are more likely the consequence of sample preparation and measurements performed on different days.

A t-test was performed on the concentration for both scatter and fluorescence for both labeled exosome samples, using the concentrations from each capture. Exosomes labeled with CMO gave a p-value of 0.741 and Exosomes labeled with Exoglow™ gave a 0.288 confirming that the scatter and fluorescence concentrations for both CMO and Exoglow™ were statistically the same using a confidence level of 0.95.

Although both dyes effectively stained urine exosomes, their photostable properties differed significantly. The fluorescence process can be interrupted or even stopped when the fluorophore is exposed to a high intensity laser light. The photostability properties are specific to individual fluorophores and can be indicative of how long the fluorescence process/signal can be

maintained. The fluorescence decay graph on the NS Xplorer software was used to assess the photostability of dyes. CMO-dyed exosomes signal was bright and more photostable under fluorescence filter than ExoGlow™ as the particles per frame from CMO-dyed exosomes remained unchanged over the capture duration, Figure 10a. As ExoGlow™ stained exosomes the fluorescence signal became dimmer the sharp decay curve was observed in the decay graph showing the particles per frame decreased with each frame, Figure 10b). Nevertheless, although visible for a very short time, the labeled exosomes were successfully tracked, sized and counted by NS Xplorer software.

Labeling the membrane of EVs is a straightforward, rapid, and effective technique commonly employed to verify the success of the purification process. However, its lack of selectivity means there is a possibility that co-purified debris may also be labeled. As a result, utilizing specific antibody labeling can offer a more reliable confirmation of EV presence.

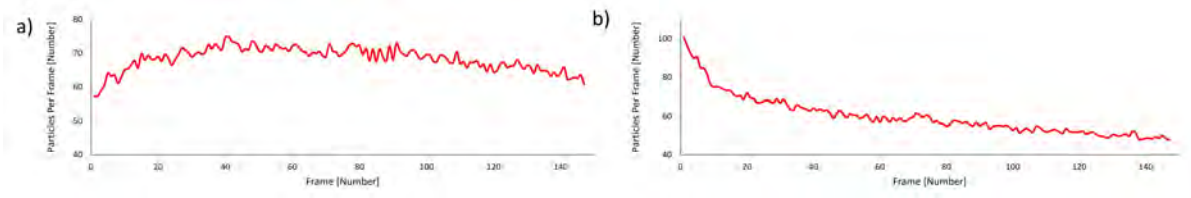

Figure 10: Fluorescence decay graphs from NS Xplorer software showing how the average particles per frame vary across the duration of the 150 frame fluorescence videos for of exosomes from urine of healthy donors labeled with a) photostable properties of CMO and b) photobleaching properties of ExoGlow™

	Control		Scatter		Fluorescence		Fluorescence efficiency [%]
	Mode [nm]	Concentration [particles/mL]	Mode [nm]	Concentration [particles/mL]	Mode [nm]	Concentration [particles/mL]	
CellMask™ Orange	77.5	3.89×10^8	92.5	2.37×10^8	97.5	2.41×10^8	102
ExoGlow™	82.5	4.46×10^8	107.5	4.56×10^8	92.5	4.39×10^8	96

Table 2: Mode (in nm) and concentration (in particles/mL) of exosomes from urine of healthy donors measured in scatter and fluorescence mode when labeled with CMO and ExoGlow™ membrane dyes using fluorescence NTA on NanoSight Pro

4.3 Specific Labeling

The fluorescence concentrations measured on the NanoSight Pro for each Alexa Fluor® 488 and PE/Cy7 dye-antibodies were used to confirm the presence of tetraspanin biomarkers within the exosomes from urine preparation and to determine the concentration of exosomes with specific surface tetraspanins. Figure 11 shows the concentrations determined from NanoSight Pro measurements under light scatter and fluorescence for exosomes from urine labeled specifically with anti-CD9, anti-CD63 and anti-CD81 antibody dyes.

The modal size and particle concentration data for Alexa Fluor® 488 and PE/Cyanine7 exosomes is shown in Table 3 along with the labeling efficiencies. EVs labeled with PE/Cyanine7 measured larger in size than EVs labeled with Alexa Fluor® 488. This may be because the PE/Cyanine7 fluorophore (molecular weight = 240 kDa, [18]) is larger than Alexa Fluor® 488 (molecular weight = 800 Da, [16]). EVs with PE/Cyanine7 attached may then have a larger diameter. However, size distribution shapes and ranges remain comparable.

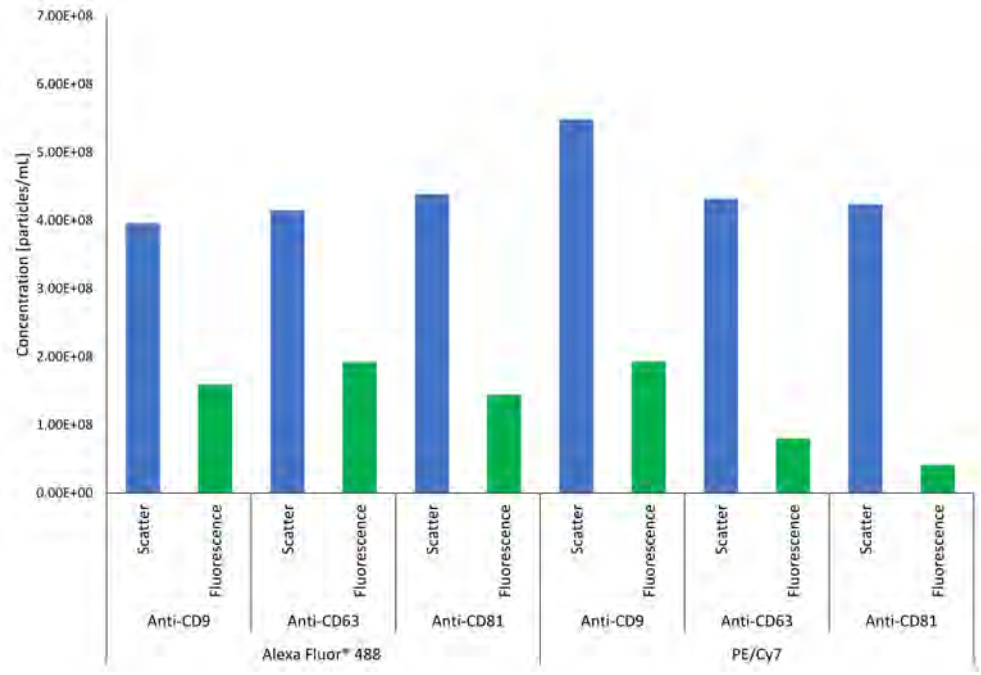

Figure 11: Particle concentrations in scatter and fluorescence measurements for exosomes labeled with Alexa Fluro 488 and PE/Cyanine7 anti-CD9, anti-CD63 and anti-CD81 antibody dyes measured using fluorescence NTA on NanoSight Pro.

		Scatter		Fluorescence	Fluorescence efficiency [%]
		Mode [nm]	Concentration [particles/mL]	Concentration [particles/mL]	
Alexa Fluor® 488	CD9	92.5	3.96×10^8	1.59×10^8	40
	CD63	87.5	4.15×10^8	1.92×10^8	46
	CD81	87.5	4.39×10^8	1.44×10^8	33
PE/Cyanine7	CD9	107.5	5.49×10^8	1.93×10^8	35
	CD63	107.5	4.32×10^8	8.00×10^7	19
	CD81	92.5	4.24×10^8	4.10×10^7	10

Table 3: Mode (in nm) and concentration (in particles/mL) of exosomes from urine of healthy donors measured in scatter and fluorescence mode when labeled with Alexa Fluor 488 and PE/Cyanine7 CD9, CD63 and CD81 antibody dyes using fluorescence NTA on NanoSight Pro

The fluorescence efficiency is a useful parameter to compare the tetraspanin concentrations for each fluorescent dye. For CD9 labeling, the reported fluorescent efficiency of 40% and 35% were achieved using Alexa488 and PE/Cyanine7 dyes, respectively. For CD63 labeling, 46% and 19% were achieved and 33% and 10% were achieved for CD81 labeling. Alexa Fluor® 488 gave higher fluorescence efficiencies than PE/Cyanine7. This may be due to the steric hindrance of PE/Cyanine7. As the fluorophores are much larger they may not be able to bind to all the tetraspanins present, giving a lower fluorescence concentration and therefore lower efficiency. Work by Oliveira-Rodríguez et al in 2016 showed that exosomes from urine of healthy donors have high concentrations of CD9 and CD63, comparing well with the reported labelling efficiencies from this study [13].

Examples of size distributions from CD9, CD63 and CD81 labeling using PE/Cyanine7 and Alexa Fluor® 488 dyes are shown in Figure 12. In all cases, the fluorescence size distributions were less concentrated than the scattering size distribution - this was as expected, and was reflected in the fluorescence efficiencies.

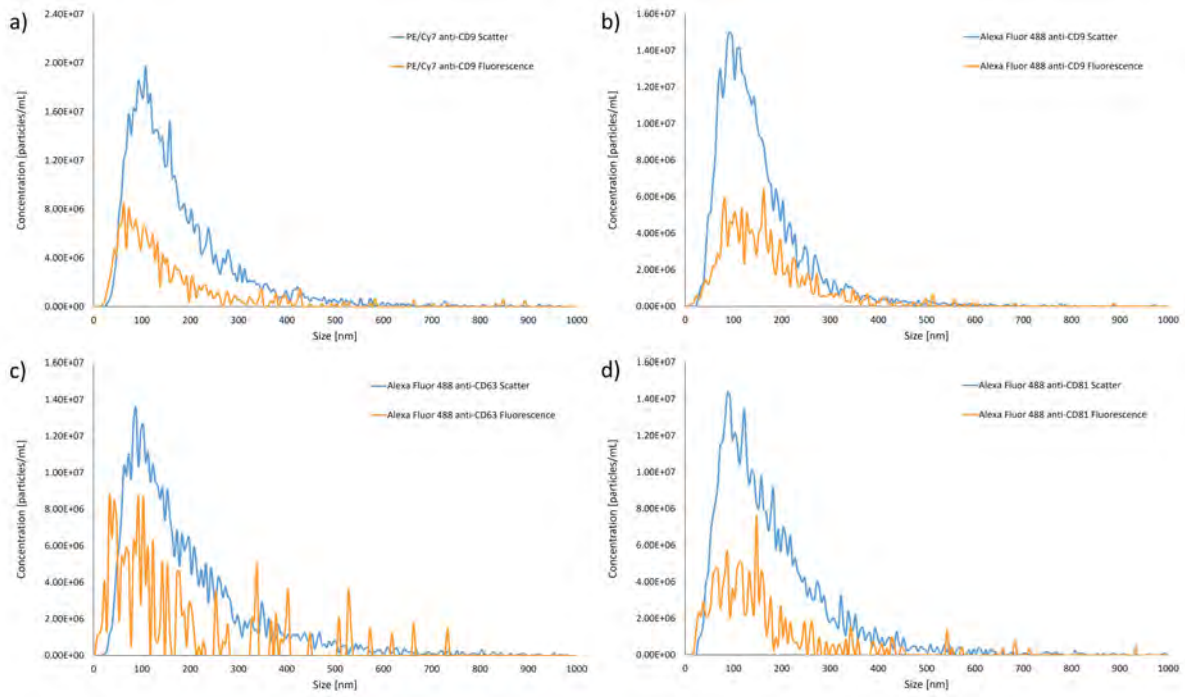

Figure 12: Size distributions of exosome from urines measured under scatter (blue) and measured under fluorescence (orange) labeled with a) PE/Cyanine7 CD9, b) Alexa 488 CD9, c) Alexa 488 CD63 and d) Alexa 488 CD81 antibody dyes.

4.4 RNA labeling

For RNA labeling, an efficiency of 54% was achieved using Quant-iT™ RiboGreen as RNA dye, meaning that around half of the exosomes likely contained RNA. A scattering concentration of 2.3 × 108 particles/mL was measured and a fluorescence concentration of 1.2 × 108 particles/mL was measured as shown in Table 4.

	Scatter		Fluorescence	Fluorescence efficiency [%]
	Mode [nm]	Concentration [particles/mL]	Concentration [particles/mL]	
Quant-iT™ RiboGreen	82.5	2.29×10^8	1.23×10^8	54

Table 4: Mode (in nm) and concentration (in particles/mL) of exosomes from urine of healthy donors measured in scatter and fluorescence mode when labeled with Quant-iT™ RiboGreen using fluorescence NTA

The size distribution is shown in Figure 13. The scatter size distribution overlaps with the control size distribution showing that the labeling hasn't affected the size distribution and concentration of the EVs. Fluorescence decay graphs from NS Xplorer software show how the average particles per frame vary across the duration of the 150 frame fluorescence videos for exosomes labeled with Quant-iT™ RiboGreen (Figure 14).

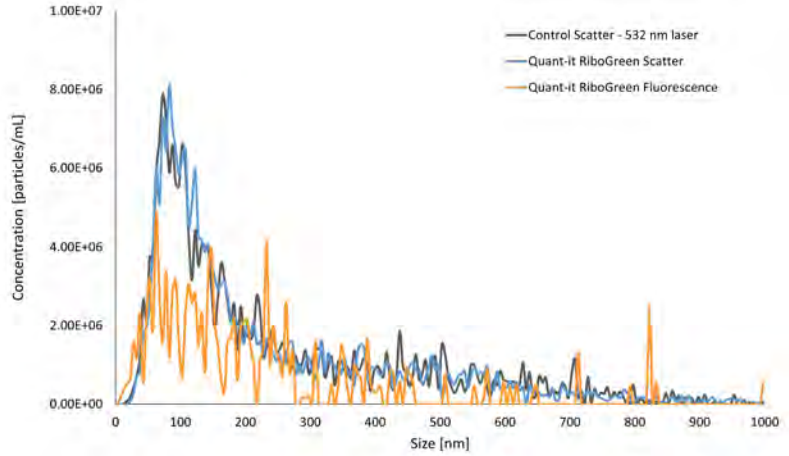

Figure 13: Scattering (blue) and fluorescence (orange) size distributions of exosomes labeled with Quant-iT™ RiboGreen RNA labeling. The control EVs size distribution is in black.

Quant-iT™ RiboGreen is relatively unphotostable as shown in Figure 14 as there is a significant decrease in the number of particles per frame.

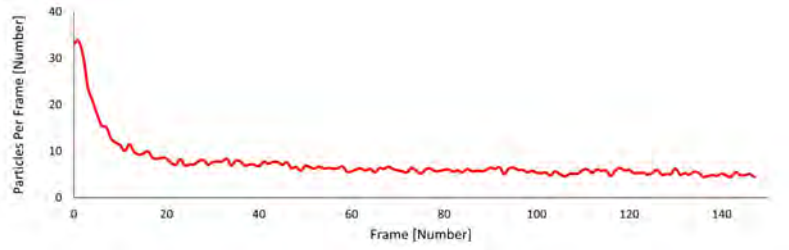

Figure 14: Fluorescence decay graphs from NS Xplorer software showing how the average particles per frame vary across the duration of the 150 frame fluorescence videos for of exosomes labeled with Quant-iT™ RiboGreen

5.0 Conclusions

NanoSight Pro has emerged as a valuable tool that is increasingly utilized in EV characterization, owing to its ability to track individual particles for both size, size distribution and concentration measurements, as well as its fluorescent mode, which facilitates exosome detection through fluorescent labeling. This whitepaper illustrates how the NanoSight Pro can be employed to explore various labeling approaches for unraveling different characteristics of EVs.

Detecting subpopulations of EVs with Fluorescence NTA is achieved by following a few simple rules concerning dye properties (e.g. photostability and brightness), sample method preparation (e.g. antibody affinity and specificity, incubation conditions) and measurement conditions (e.g. sample presentation, instrument settings, measurement duration).

Initially, urine-derived extracellular vesicles (EVs) were effectively characterized in terms of size, heterogeneity of size distribution and concentration, serving as control measurements. Furthermore, successful membrane labeling was demonstrated using two different fluorescent dyes with distinct photostabilities (CellMask™ Orange and ExoGlow™). Both dyes exhibited approximately 100% labeling efficiencies, confirming the presence and purity of urine-derived EVs and showcasing the NanoSight Pro's capability to accurately measure fluorescence signals, even from more photobleaching dyes like Exoglow. Biomarker detection methods were then developed using two different dyes, Alexa Fluor® 488 (488 nm excitation wavelength) and Pe/Cyanine (either 488 or 532 nm excitation wavelength). With both dyes, the presence of CD9, CD63, and CD81 biomarkers was confirmed, with Alexa Fluor® 488 yielding slightly higher fluorescence labeling efficiencies due to the different properties between the two dyes. Finally, the cargo detection method was successfully established, using the Quant-iT™ RiboGreen dye, revealing an RNA labeling efficiency of 52%.

To conclude, as extensively demonstrated, the NanoSight Pro, with its specialized fluorescence mode, holds limitless capacity in advancing research and development efforts concerning extracellular vesicles (EVs) for both diagnostic and

treatment applications.

6.0 References

1. György, B., Hung, M. E., Breakefield, X. O., & Leonard, J. N. (2015). Therapeutic Applications of Extracellular Vesicles: Clinical Promise and Open Questions. Annual Review of Pharmacology and Toxicology, 55(1), 439–464.

2. Welsh, J.A., et al, Lange, S., Misev Consortium, Théry, C. and Witwer, K.W. 2024. Minimal information for studies of extracellular vesicles (MISEV2023): From basic to advanced approaches. Journal of Extracellular Vesicles. 13 (2) e12404.

3. Barteneva, N. S., Fasler-Kan, E., Bernimoulin, M., Stern, J. N., Ponomarev, E. D., Duckett, L., & Vorobjev, I. A. (2013). Circulating microparticles: square the circle. BMC Cell Biology, 14(1), 23.

4. Ciferri, M. C., Quarto, R., & Tasso, R. (2021). Extracellular Vesicles as Biomarkers and Therapeutic Tools: From Pre-Clinical to Clinical Applications. Biology, 10(5), 359. https://doi.org/10.3390/biology10050359

5. Mathieu, M., Névo, N., Jouve, M., Valenzuela, J. I., Maurin, M., Verweij, F. J., Palmulli, R., Lankar, D., Dingli, F., Loew, D., Rubinstein, E., Boncompain, G., Perez, F., & Théry, C. (2021). Specificities of exosome versus small ectosome secretion revealed by live intracellular tracking of CD63 and CD9. Nature Communications, 12(1), 4389.

6. Jankovičová, J., Sečová, P., Michalková, K., & Antalíková, J. (2020). Tetraspanins, More than Markers of Extracellular Vesicles in Reproduction. International Journal of Molecular Sciences, 21(20), 7568.

7. Wang, J., Yue, B.-L., Huang, Y.-Z., Lan, X.-Y., Liu, W.-J., & Chen, H. (2022). Exosomal RNAs: Novel Potential Biomarkers for Diseases—A Review. International Journal of Molecular Sciences, 23(5), 2461. https://doi.org/10.3390/ijms23052461

8. Van Der Pol, E., Hoekstra, A. G., Sturk, A., Otto, C., Van Leeuwen, T. G., & Nieuwland, R. (2010). Optical and non-optical methods for detection and characterization of microparticles and exosomes. Journal of Thrombosis and Haemostasis, 8(12), 2596–2607.

9. Kurian, T. K., Banik, S., Gopal, D., Chakrabarti, S., & Mazumder, N. (2021). Elucidating Methods for Isolation and Quantification of Exosomes: A Review. Molecular Biotechnology, 63(4), 249–266.

10. Dragovic, R. A., Gardiner, C., Brooks, A. S., Tannetta, D. S., Ferguson, D. J. P., Hole, P., Carr, B., Redman, C. W. G., Harris, A. L., Dobson, P. J., Harrison, P., & Sargent, I. L. (2011). Sizing and phenotyping of cellular vesicles using Nanoparticle Tracking Analysis. Nanomedicine: Nanotechnology, Biology and Medicine, 7(6), 780–788.

11. Ragheb, R., Siupa, A., & Ashley, L. (2023, November 23). Nanoparticle Tracking Analysis with Confidence! - The use of Machine Learning with the NanoSight Pro - Materials Talks. https://www.malvernpanalytical.com/en/learn/knowledge-center/insights/nanoparticle-tracking-analysis-with-confidence-the-use-of-machine-learning-with-the-nanosight-pro

12. Thane, K. E., Davis, A. M., & Hoffman, A. M. (2019). Improved methods for fluorescent labeling and detection of single extracellular vesicles using nanoparticle tracking analysis. Scientific Reports, 9(1), 12295.

13. Oliveira-Rodríguez, M., López-Cobo, S., Reyburn, H. T., Costa-García, A., López-Martín, S., Yáñez-Mó, M., Cernuda-Morollón, E., Paschen, A., Valés-Gómez, M., & Blanco-López, M. C. (2016). Development of a rapid lateral flow immunoassay test for detection of exosomes previously enriched from cell culture medium and body fluids. Journal of Extracellular Vesicles, 5(1), 31803.

14. Carnell-Morris, P., Tannetta, D., Siupa, A., Hole, P., & Dragovic, R. (2017). Analysis of Extracellular Vesicles Using Fluorescence Nanoparticle Tracking Analysis. In W. P. Kuo & S. Jia (Eds.), Extracellular Vesicles (Vol. 1660, pp. 153–173). Springer New York.

15. HansaBiomed. Retrieved 13 March 2024, from https://hansabiomed.eu/shop/image/catalog/Inserts/Exo%20standards.pdf

16. FluoroFinder. (n.d.-a). Retrieved 26 February 2024, from https://app.fluorofinder.com/dyes/5-alexa-fluor-488-ex-max-490-nm-em-max-525-nm

17. ExoGlowTM-Membrane EV Labeling Kit. (n.d.). Retrieved 26 February 2024, from https://www.systembio.com/products/exosome-research/exosome-labeling/exoglow/exoglow-membrane-ev-labeling-kit

18. FluoroFinder. (n.d.-b). Retrieved 26 February 2024, from https://app.fluorofinder.com/dyes/35-pe-cy7-ex-max-565-nm-em-max-778-nm

19. FluoroFinder. (n.d.-c). Retrieved 26 February 2024, from https://app.fluorofinder.com/dyes/1615-cellmask-orange-plasma-membrane-stain-ex-max-556-nm-em-max-571-nm

20. Quant-itTM RiboGreen RNA Assay Kit and RiboGreen RNA Reagent, RediPlateTM 96 RiboGreenTM RNA Quantitation Kit. (n.d.). Retrieved 26 February 2024, from https://www.thermofisher.com/order/catalog/product/R11490

21. Igami, K., Uchiumi, T., Shiota, M., Ueda, S., Tsukahara, S., Akimoto, M., Eto, M., & Kang, D. (2022). Extracellular vesicles expressing CEACAM proteins in the urine of bladder cancer patients. Cancer Science, 113(9), 3120–3133.

Edition notice

First Edition, April 2024

MALVERN PANALYTICAL

Grovewood Road, Malvern
Worcestershire, WR14 1XZ
United Kingdom
Tel. +44 1684 892456
Fax. +44 1684 892789

Lelyweg 1,
7602 EA Almelo,
The Netherlands
Tel. +31 546 534 444
Fax. +31 546 534 598